Historic England

Marden Henge, Marden, Wiltshire

Optical Dating of Sediments

Phil Toms, Martin Bell and Jamie Wood

Discovery, Innovation and Science in the Historic Environment

Research Report Series no. 75/2018

Research Report Series 75-2018

MARDEN HENGE
MARDEN
WILTSHIRE

OPTICAL DATING OF SEDIMENTS

Phil Toms, Martin Bell and Jamie Wood

NGR: SU 0919 5791

ISSN 2059-4453 (Online)

The Research Report Series incorporates reports by the expert teams within the Investigation & Analysis Division of the Heritage Protection Department of Historic England, alongside contributions from other parts of the organisation. It replaces the former Centre for Archaeology Reports Series, the Archaeological Investigation Report Series, the Architectural Investigation Report Series, and the Research Department Report Series.

Many of the Research Reports are of an interim nature and serve to make available the results of specialist investigations in advance of full publication. They are not usually subject to external refereeing, and their conclusions may sometimes have to be modified in the light of information not available at the time of the investigation. Where no final project report is available, readers must consult the author before citing these reports in any publication. Opinions expressed in Research Reports are those of the author(s) and are not necessarily those of Historic England.

For more information write to Res.reports@HistoricEngland.org.uk
or mail: Historic England, Fort Cumberland, Fort Cumberland Road, Eastney, Portsmouth PO4 9LD

SUMMARY
Optically Stimulated Luminescence (OSL) dating of the organic-poor sands immediately adjacent to the late Neolithic henge bank at Marden demonstrated that the sediments pre-date the construction of the feature.

CONTRIBUTORS
Phil Toms, Luminescence dating laboratory, School of Natural & Social Sciences, University of Gloucestershire, Swindon Road, Cheltenham GL50 4AZ
Martin Bell, Department of Archaeology, University of Reading, Whiteknights, PO Box 227, Reading RG6 6AH
Jamie Wood, Luminescence dating laboratory, School of Natural & Social Sciences, University of Gloucestershire, Swindon Road, Cheltenham GL50 4AZ

ACKNOWLEDGEMENTS
The cover photo is © Historic England. NMR 24502_009 taken on 6 December 2006 by Damian Grady.

ARCHIVE LOCATION
Wiltshire Archaeology Service, The Wiltshire and Swindon History Centre, Cocklebury Road, Chippenham, SN15 3QN

DATE OF RESEARCH
2018

CONTACT DETAILS
Phil Toms, Luminescence dating laboratory, School of Natural & Social Sciences, University of Gloucestershire, Swindon Road, Cheltenham GL50 4AZ.
Tel: 01242 714708
Email: ptoms@glos.ac.uk

CONTENTS

INTRODUCTION

Henge monuments are enigmatic features of late Neolithic Britain. Formed by a ring-bank and ditch, they were used for significant ceremonial or ritual activity. Marden henge in Wiltshire (Fig 1) is one of Britain's most important, but least understood, prehistoric monuments (Leary and Field 2012). Its pronounced scale (15.7ha) makes it the largest Neolithic henge in Britain (Fig 2). It is also notable for two unusual features; a large conical mound known as the Hatfield Barrow and an inner henge (Field *et al* 2009). In collaboration with Historic England the University of Reading's Archaeology Field School excavated the Marden henge from 2015–17 as part of their Vale of Pewsey project, which focuses upon the ancient land between the iconic prehistoric monuments of Stonehenge and Avebury. One aim of the Marden excavations was to establish the chronological relationship between the henge and Pewsey Vale sediment sequence. To that end Trench 1a (Fig 3) was sampled in 2017 for Optically Stimulated Luminescence (OSL) dating of the organic-poor sands immediately adjacent to the henge.

MECHANISMS AND PRINCIPLES OF LUMINESCENCE DATING

Upon exposure to ionising radiation, electrons within the crystal lattice of insulating minerals are displaced from their atomic orbits. Whilst this dislocation is momentary for most electrons, a portion of charge is redistributed to meta-stable sites (traps) within the crystal lattice. In the absence of significant optical and thermal stimuli, this charge can be stored for extensive periods. The quantity of charge relocation and storage relates to the magnitude and period of irradiation. When the lattice is optically or thermally stimulated, charge is evicted from traps and may return to a vacant orbit position (hole). Upon recombination with a hole, an electron's energy can be dissipated in the form of light generating crystal luminescence providing a measure of dose absorption.

Herein, quartz is segregated for dating. The utility of this minerogenic dosimeter lies in the stability of its datable signal over the mid–late Quaternary period, predicted through isothermal decay studies (eg Smith *et al* 1990; retention lifetime 630Ma at 20°C) and evidenced by optical age estimates concordant with independent chronological controls (eg Murray and Olle, 2002). This stability is in contrast to the anomalous fading of comparable signals commonly observed for other ubiquitous sedimentary minerals such as feldspar and zircon (Wintle 1973; Templer 1985; Spooner 1993).

Optical age estimates of sedimentation (Huntley *et al* 1985) are premised upon reduction of the minerogenic time dependent signal (OSL) to zero through exposure to sunlight and, once buried, signal reformulation by absorption of litho- and cosmogenic radiation. The signal accumulated post-burial acts as a dosimeter recording total dose absorption, converting to a chronometer by estimating the rate of dose absorption quantified through the assay of radioactivity in the surrounding lithology and streaming from the cosmos.

$$\text{Age} = \frac{\text{Mean Equivalent Dose } (D_e, \text{Gy})}{\text{Mean Dose Rate } (D_r, \text{Gy.ka}^{-1})}$$

Aitken (1998) and Bøtter-Jensen *et al* (2003) offer a detailed review of optical dating.

SAMPLE COLLECTION AND PREPARATION

Three sediment samples were collected in section using opaque tubing (Fig 1, Table 1), each from a separate context. Context 1041 (Lab Code GL17061) was a sandy marl sediment overlying Pleistocene gravel, context 1042 (Lab Code GL17062) a marl interleaved with organic silts representing a former land surface, and context 1043 (Lab Code GL17063) was a sandy sediment interpreted as colluvium from the adjacent slope that formed part of the Marden henge.

To preclude optical erosion of the datable signal prior to measurement, all samples were opened and prepared under controlled laboratory illumination provided by Encapsulite RB-10 (red) filters. To isolate that material potentially exposed to daylight during sampling, sediment located within 20mm of each tube-end was removed.

The remaining sample was dried and then sieved. The fine sand fraction was segregated and subjected to acid and alkaline digestion (10% HCl, 15% H_2O_2) to attain removal of carbonate and organic components respectively. A further acid digestion in HF (40%, 60mins) was used to etch the outer 10-15μm layer affected by α radiation and degrade each samples' feldspar content. During HF treatment, continuous magnetic stirring was used to affect isotropic etching of grains. 10% HCl was then added to remove acid soluble fluorides. Each sample was dried, resieved and quartz isolated from the remaining heavy mineral fraction using a sodium polytungstate density separation at 2.68g.cm^{-3}. Twelve 8mm multi-grain aliquots (*c* 3–6mg) of quartz from each sample were then mounted on aluminium discs for determination of D_e values.

All drying was conducted at 40°C to prevent thermal erosion of the signal. All acids and alkalis were Analar grade. All dilutions (removing toxic-corrosive and non-minerogenic, luminescence-bearing substances) were conducted with distilled water to prevent signal contamination by extraneous particles.

ACQUISITION AND ACCURACY OF D_E VALUE

All minerals naturally exhibit marked inter-sample variability in luminescence per unit dose (sensitivity). Therefore, the estimation of D_e acquired since burial requires calibration of the natural signal using known amounts of laboratory dose. D_e values were quantified using a single-aliquot regenerative-dose (SAR) protocol (Murray and Wintle 2000; 2003) facilitated by a Risø TL-DA-15 irradiation-stimulation-detection system (Markey *et al* 1997; Bøtter-Jensen *et al* 1999). Within this apparatus, optical signal stimulation is provided by an assembly of blue diodes (five packs of six Nichia NSPB500S), filtered to 470±80nm conveying 15mW.cm^{-2} using a 3mm Schott GG420 positioned in front of each diode pack. Infrared (IR) stimulation, provided by six IR diodes (Telefunken TSHA 6203) stimulating at 875±80nm delivering ~5mW.cm^{-2}, was used to indicate the presence of contaminant feldspars (Hütt *et al* 1988). Stimulated photon emissions from quartz aliquots are in the ultraviolet (UV) range and were filtered from stimulating photons

by 7.5mm HOYA U-340 glass and detected by an EMI 9235QA photomultiplier fitted with a blue-green sensitive bialkali photocathode. Aliquot irradiation was conducted using a 1.48 GBq $^{90}Sr/^{90}Y$ β source calibrated for multi-grain aliquots of 125–180μm quartz against the 'Hotspot 800' ^{60}Co γ source located at the National Physical Laboratory (NPL), UK.

SAR by definition evaluates D_e through measuring the natural signal (Appendices 1–3: Fig i) of a single aliquot and then regenerating that aliquot's signal by using known laboratory doses to enable calibration. For each aliquot, five different regenerative-doses were administered so as to image dose response. D_e values for each aliquot were then interpolated, and associated counting and fitting errors calculated, by way of exponential plus linear regression (Appendices 1–3: Fig i). Weighted (geometric) mean D_e values were calculated from 12 aliquots using the central age model outlined by Galbraith *et al* (1999) and are quoted at 1σ confidence (Table 1). The accuracy with which D_e equates to total absorbed dose and that dose absorbed since burial was assessed. The former can be considered a function of laboratory factors, the latter, one of environmental issues. Diagnostics were deployed to estimate the influence of these factors and criteria instituted to optimise the accuracy of D_e values.

LABORATORY FACTORS

Feldspar contamination

The propensity of feldspar signals to fade and underestimate age, coupled with their higher sensitivity relative to quartz makes it imperative to quantify feldspar contamination. At room temperature, feldspars generate a signal (IRSL; Appendices 1–3: Fig i) upon exposure to IR whereas quartz does not. The signal from feldspars contributing to OSL can be depleted by prior exposure to IR. For all aliquots the contribution of any remaining feldspars was estimated from the OSL IR depletion ratio (Duller 2003). The influence of IR depletion on the OSL signal can be illustrated by comparing the regenerated post-IR OSL D_e with the applied regenerative-dose. If the addition to OSL by feldspars is insignificant, then the repeat dose ratio of OSL to post-IR OSL should be statistically consistent with unity. This is the case for the entire OSL sample suite at Marden (Table 1) and, therefore, feldspar contamination is not a concern.

Preheating

Preheating aliquots between irradiation and optical stimulation is necessary to ensure comparability between natural and laboratory-induced signals. However, the multiple irradiation and preheating steps that are required to define single-aliquot regenerative-dose response leads to signal sensitisation, rendering calibration of the natural signal inaccurate. The SAR protocol (Murray and Wintle 2000, 2003) enables this sensitisation to be monitored and corrected using a test dose, here set at 5Gy preheated to 220°C for 10s, to track signal sensitivity between irradiation-preheat steps. However, the accuracy of sensitisation correction for both natural and laboratory signals can be preheat dependent.

The Dose Recovery test was used to assess the optimal preheat temperature for accurate correction and calibration of the time dependent signal. Dose Recovery

(Appendices 1–3: Fig ii) attempts to quantify the combined effects of thermal transfer and sensitisation on the natural signal, using a precise lab dose to simulate natural dose. The ratio between the applied dose and recovered D_e value should be statistically concordant with unity. For this diagnostic, six aliquots were each assigned a 10s preheat between 180°C and 280°C.

Preheat treatments of 260°C for GL17061 and GL17062 and 240°C for GL17063 fulfilled the criterion of accuracy within the Dose Recovery test, and were selected to generate the final D_e value from a further 12 aliquots. Further thermal treatments, prescribed by Murray and Wintle (2000; 2003), were applied to optimise accuracy and precision. Optical stimulation occurred at 125°C in order to minimise effects associated with photo-transferred thermoluminescence and maximise signal to noise ratios. Inter-cycle optical stimulation was conducted at 280°C to minimise recuperation.

Internal consistency

Abanico plots (Dietze *et al* 2016) are used to illustrate inter-aliquot D_e variability (Appendices 1–3: Fig iii). D_e values are standardised relative to the central D_e value for natural signals and are described as over-dispersed when >5% lie beyond $\pm 2\sigma$ of the standardising value; resulting from a heterogeneous absorption of burial dose and/or response to the SAR protocol. For multi-grain aliquots, over-dispersion of natural signals does not necessarily imply inaccuracy. However where over-dispersion is observed for regenerated signals, the efficacy of sensitivity correction may be problematic. Murray and Wintle (2000; 2003) suggest repeat dose ratios offer a measure of SAR protocol success, whereby ratios ranging across 0.9–1.1 are acceptable. However, this variation of repeat dose ratios in the high-dose region can have a significant impact on D_e interpolation. The influence of this effect can be outlined by quantifying the ratio of interpolated to applied regenerative-dose ratio. Since both the repeat dose ratios and interpolated to applied regenerative-dose ratios range across 0.9–1.1 in this study (Table 1), sensitivity-correction is considered effective.

ENVIRONMENTAL FACTORS

Incomplete zeroing

Post-burial OSL signals residual of pre-burial dose absorption can result where pre-burial sunlight exposure is limited in spectrum, intensity and/or period, leading to age overestimation. This effect is particularly acute for material eroded and redeposited sub-aqueously (Olley *et al* 1998, 1999; Wallinga 2002) and exposed to a burial dose of <20Gy (eg Olley *et al* 2004), has some influence in sub-aerial contexts but is rarely of consequence where aerial transport has occurred. Within single-aliquot regenerative-dose optical dating there are two diagnostics of partial resetting (or bleaching); signal analysis (Agersnap-Larsen *et al* 2000; Bailey *et al* 2003) and inter-aliquot D_e distribution studies (Murray *et al* 1995).

Within this study, signal analysis was used to quantify the change in D_e value with respect to optical stimulation time for multi-grain aliquots. This exploits the existence of traps within minerogenic dosimeters that bleach with different efficiency for a given wavelength of light to verify partial bleaching. D_e (t) plots

(Appendices 1–3: Fig iv; Bailey *et al* 2003) are constructed from separate integrals of signal decay as laboratory optical stimulation progresses. A statistically significant increase in natural D_e (t) is indicative of partial bleaching assuming three conditions are fulfilled. Firstly, that a statistically significant increase in D_e (t) is observed when partial bleaching is simulated within the laboratory. Secondly, that there is no significant rise in D_e (t) when full bleaching is simulated. Finally, there should be no significant augmentation in D_e (t) when zero dose is simulated. Where partial bleaching is detected, the age derived from the sample should be considered a maximum estimate only. However, the utility of signal analysis is strongly dependent upon a samples pre-burial experience of sunlight's spectrum and it's residual to post-burial signal ratio. Given in the majority of cases, the spectral exposure history of a deposit is uncertain, the absence of an increase in natural D_e (t) for the Marden OSL samples does not necessarily testify to the absence of partial bleaching.

The insensitivities of multi-grain single-aliquot signal analysis may be circumvented by inter-aliquot D_e distribution studies of the Marden sequence in the event of further sampling campaigns. This analysis uses aliquots of single sand grains to quantify inter-grain D_e distribution. At present, it is contended that asymmetric inter-grain D_e distributions are symptomatic of partial bleaching and/or pedoturbation (Murray *et al* 1995; Olley *et al* 1999, 2004; Bateman *et al* 2003). For partial bleaching at least, it is further contended that the D_e acquired during burial is located in the minimum region of such ranges. The mean and breadth of this minimum region is the subject of current debate, as it is additionally influenced by heterogeneity in micro-dosimetry, variable inter-grain response to SAR and residual to post-burial signal ratios.

Turbation

As noted above, the accuracy of sedimentation ages can further be controlled by post-burial trans-strata grain movements forced by cryo- or pedoturbation. Inaccuracy forced by cryoturbation may be bidirectional, heaving older material upwards or drawing younger material downwards into the level to be dated. Cryogenic deformation of matrix-supported material is, typically, visible; there are no signs of this within the Marden units sampled for OSL dating. Berger (2003) contends pedogenesis prompts a reduction in the apparent sedimentation age of parent material through bioturbation and illuviation of younger material from above and/or by biological recycling and resetting of the datable signal of surface material. Berger (2003) proposes that the chronological products of this remobilisation are A-horizon age estimates reflecting the cessation of pedogenic activity, Bc/C-horizon ages delimiting the maximum age for the initiation of pedogenesis with estimates obtained from Bt-horizons providing an intermediate age 'close to the age of cessation of soil development'. Singhvi *et al* (2001), in contrast, suggest that B and C-horizons closely approximate the age of the parent material, the A-horizon, that of the 'soil forming episode'. Recent analyses of inter-aliquot D_e distributions have reinforced this complexity of interpreting burial age from pedoturbated deposits (Lombard *et al* 2011; Gliganic *et al* 2015, 2016; Jacobs *et al* 2008; Bateman *et al* 2007). At present there is no definitive post-sampling mechanism for the direct detection of and correction for post-burial sediment remobilisation. However, intervals of palaeosol evolution can be delimited by a maximum age derived from

parent material and a minimum age obtained from a unit overlying the palaeosol. In this sense, the age of the palaeosol represented by context 1042 may be best approximated by the underlying sample GL17061 and the overlying sample GL17063, though this is perhaps immaterial given the lack of statistical distinction in age.

ACQUISITION AND ACCURACY OF D_R VALUE

Lithogenic D_r values were defined through measurement of U, Th and K radionuclide concentration and conversion of these quantities into β and γ D_r values (Table 1). β contributions were estimated from sub-samples by laboratory-based γ spectrometry using an Ortec GEM-S high purity Ge coaxial detector system, calibrated using certified reference materials supplied by CANMET. γ dose rates can be estimated from *in situ* NaI gamma spectrometry or, where direct measurements are unavailable as in the present case, from laboratory-based Ge γ spectrometry. *In situ* measurements reduce uncertainty relating to potential heterogeneity in the γ dose field surrounding each sample. The level of U disequilibrium was estimated by laboratory-based Ge γ spectrometry. Estimates of radionuclide concentration were converted into D_r values (Adamiec and Aitken 1998), accounting for D_r modulation forced by grain size (Mejdahl 1979) and present moisture content (Zimmerman 1971). Cosmogenic D_r values were calculated on the basis of sample depth, geographical position and matrix density (Prescott and Hutton 1994).

The spatio-temporal validity of D_r values can be considered a function of five variables. Firstly, age estimates devoid of *in situ* γ spectrometry data should be accepted tentatively if the sampled unit is heterogeneous in texture or if the sample is located within 300mm of strata consisting of differing texture and/or mineralogy. At Marden, where the three samples are vertically spaced within 200mm of each other, the consistency of γ D_r values based solely on laboratory measurements evidences the homogeneity of the γ field and hence accuracy of γ D_r values. Secondly, disequilibrium can force temporal instability in U and Th emissions. The impact of this phenomenon (Olley *et al* 1996) upon age estimates is usually insignificant given their associated margins of error. However, for samples where this effect is pronounced (>50% disequilibrium between ^{238}U and ^{226}Ra; Appendices 1–3: Fig v), the resulting age estimates should be accepted tentatively. In the case of GL16063 U disequilibrium appears significant, with an excess of ^{226}Ra (Appendix 3: Fig v). Consequently, the total D_r value for this sample (Table 1) is potentially a slight underestimate and the age for GL17063, therefore, might be considered a maximum age estimate. Thirdly, pedogenically-induced variations in matrix composition of B and C-horizons, such as radionuclide and/or mineral remobilisation, may alter the rate of energy emission and/or absorption. Since D_r is invariant through the dated profile at Marden and the samples encompass primary parent material, then element mobility is likely limited in effect. Fourthly, spatio-temporal detractions from present moisture content are difficult to assess directly, requiring knowledge of the magnitude and timing of differing contents. However, the maximum influence of moisture content variations can be delimited by recalculating D_r for minimum (zero) and maximum (saturation) content. Finally, temporal alteration in the thickness of overburden alters cosmic D_r values. Cosmic D_r often forms a negligible portion of total D_r. It is possible to quantify the

maximum influence of overburden flux by recalculating D_r for minimum (zero) and maximum (surface sample) cosmic D_r. The maximum influence of temporal variations in D_r forced by minima-maxima in moisture content and overburden thickness is illustrated in Figure vi, Appendices 1–3.

ESTIMATION OF AGE

Ages reported in Table 1 provide an estimate of sediment burial period based on mean D_e and D_r values and their associated analytical uncertainties. Uncertainty in age estimates is reported as a product of systematic and experimental errors, with the magnitude of experimental errors alone shown in parenthesis (Table 1). Cumulative frequency plots indicate the inter-aliquot variability in age (Appendices 1–3; Fig vi).

ANALYTICAL UNCERTAINTY

All errors are based upon analytical uncertainty and quoted at 1σ confidence. Error calculations account for the propagation of systematic and/or experimental (random) errors associated with D_e and D_r values.

For D_e values, systematic errors are confined to laboratory β source calibration. Uncertainty in this respect is that combined from the delivery of the calibrating γ dose (1.2%; NPL, pers. comm.), the conversion of this dose for SiO_2 using the respective mass energy-absorption coefficient (2%; Hubbell 1982) and experimental error, totalling 3.5%. Mass attenuation and bremsstrahlung losses during γ dose delivery are considered negligible. Experimental errors relate to D_e interpolation using sensitisation corrected dose responses. Natural and regenerated sensitisation corrected dose points (Si) were quantified by,

$$Si = (D_i - x.L_i) / (d_i - x.L_i) \qquad \textbf{Eq.1}$$

where D_i = Natural or regenerated OSL, initial 0.2s
L_i = Background natural or regenerated OSL, final 5s
d_i = Test dose OSL, initial 0.2s
x = Scaling factor, 0.08

The error on each signal parameter is based on counting statistics, reflected by the square-root of measured values. The propagation of these errors within Eq. 1 generating σSi follows the general formula given in Eq. 2. σSi were then used to define fitting and interpolation errors within exponential plus linear regressions.

For D_r values, systematic errors accommodate uncertainty in radionuclide conversion factors (5%), β attenuation coefficients (5%), a-value (4%; derived from a systematic α source uncertainty of 3.5% and experimental error), matrix density ($0.20 g.cm^{-3}$), vertical thickness of sampled section (specific to sample collection device), saturation moisture content (3%), moisture content attenuation (2%) and burial moisture content (25% relative, unless direct evidence exists of the magnitude and period of differing content). Experimental errors are associated with radionuclide quantification for each sample by Ge gamma spectrometry.

The propagation of these errors through to age calculation was quantified using the expression,

$$\sigma y\,(\delta y/\delta x) = (\sum ((\delta y/\delta x_n).\sigma x_n)^2)^{1/2} \qquad \text{Eq. 2}$$

where y is a value equivalent to that function comprising terms x_n and where σy and σx_n are associated uncertainties.

Errors on age estimates are presented as combined systematic and experimental errors and experimental errors alone. The former (combined) error should be considered when comparing luminescence ages herein with independent chronometric controls. The latter assumes systematic errors are common to luminescence age estimates generated by means identical to those detailed herein and enable direct comparison with those estimates.

SYNOPSIS

In respect of the D_e value for each of the three OSL samples, there was no significant feldspar contamination, the preheat temperature selected assured compatibility between natural and laboratory irradiated signals, and changes in signal sensitivity during the measurement process were accurately corrected. Given that the deposits are younger than 20ka and that the modes of deposition (waterlain or slope-derived) may limit exposure to sunlight prior to burial, partial bleaching and thus age overestimation cannot be ruled out. This could be explored further through inter-grain D_e analysis. However, the OSL age estimates are consistent with their relative stratigraphic positions, thus the impact of partial bleaching is likely to be limited. Sample GL17062 was obtained from a palaeosol, hence its age may best be bracketed by those from GL17061 and GL17063. However, this is inconsequential given the age for GL17062 is coeval with these under and overlying samples. Assessment of D_r variables suggests that the gamma field across the sampled units is homogenous and that, therefore, the absence of *in situ* measurements of gamma is not a concern. The invariability of D_r between the three samples suggests element mobility was limited. Significant U disequilibrium was observed for GL17063, with the excess in ^{226}Ra likely translating to a slight overestimation of age but still likely placing this unit within the early Mesolithic. Even with extreme values for overburden and moisture content, deposition of the sediments sampled at the Marden henge was firmly earlier than the Neolithic.

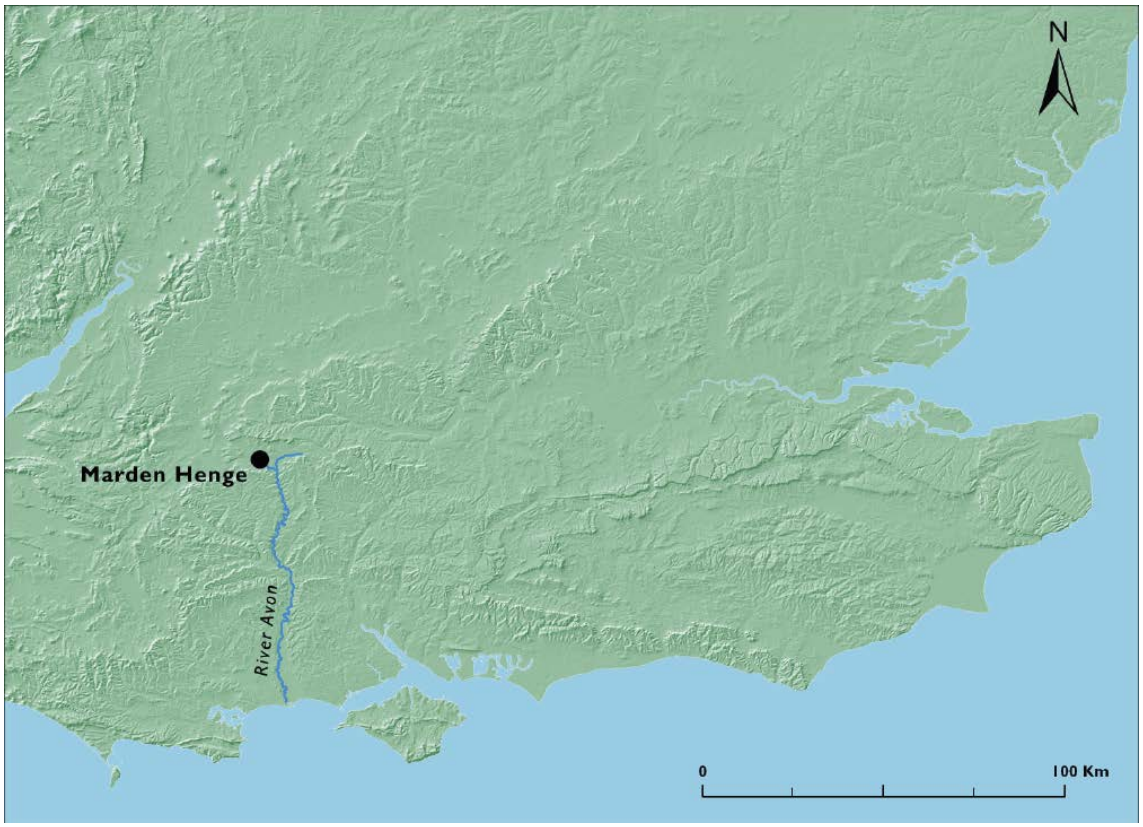

Figure 1:Map showing the location of Marden Henge

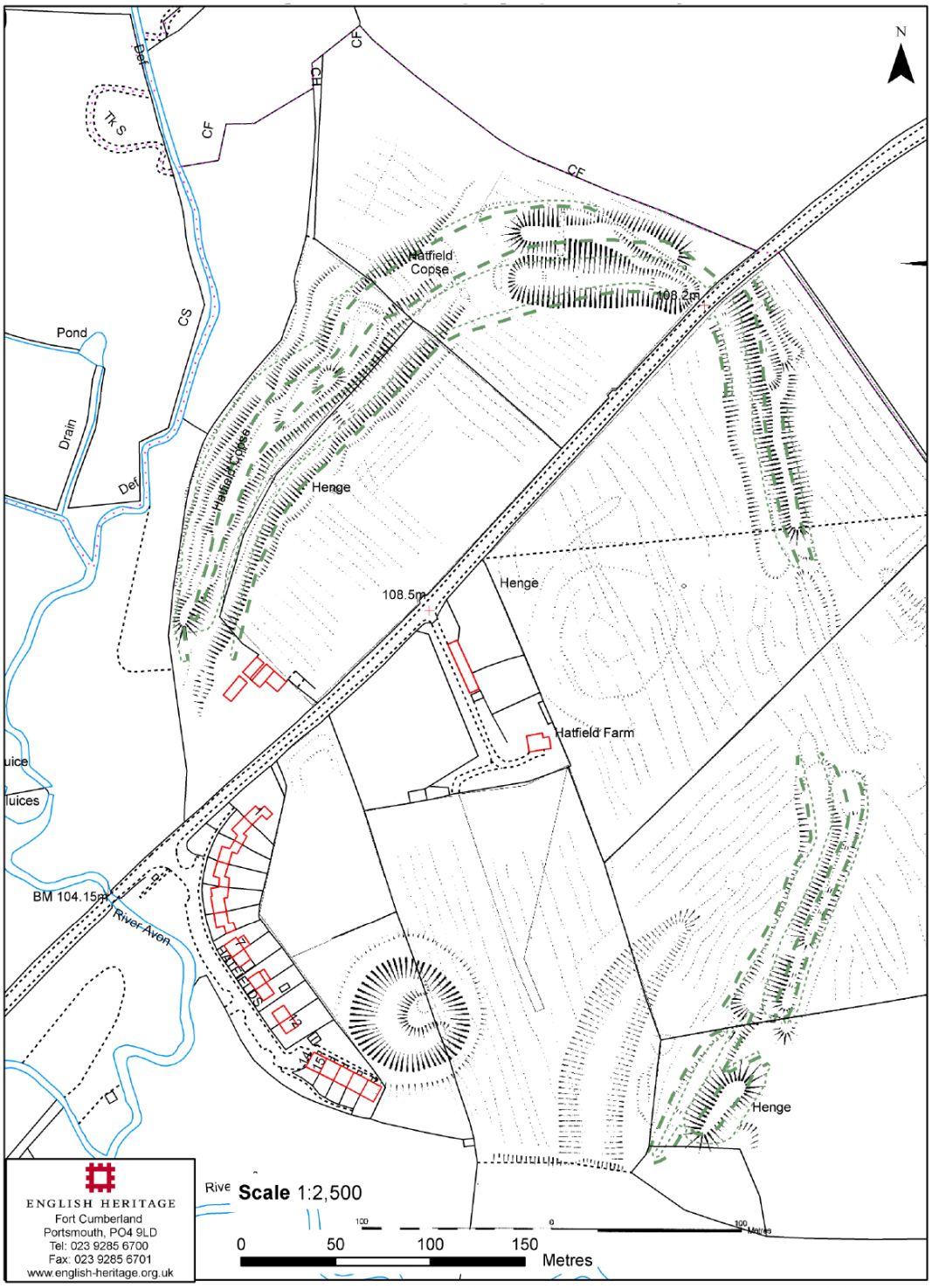

Ordnance Survey Mapping: ©Crown Copyright and database right 2010. All rights reserved. Ordnance Survey Licence number 100019088.
Historic OS Maps: © and database right Crown Copyright and Landmark Information Group Ltd (All rights reserved) License numbers 000394 and TP0024.
Elevation and colour vertical aerial photography data licensed to English Heritage for PGA through Next Perspectives™

Figure 2: Plan of Marden Henge

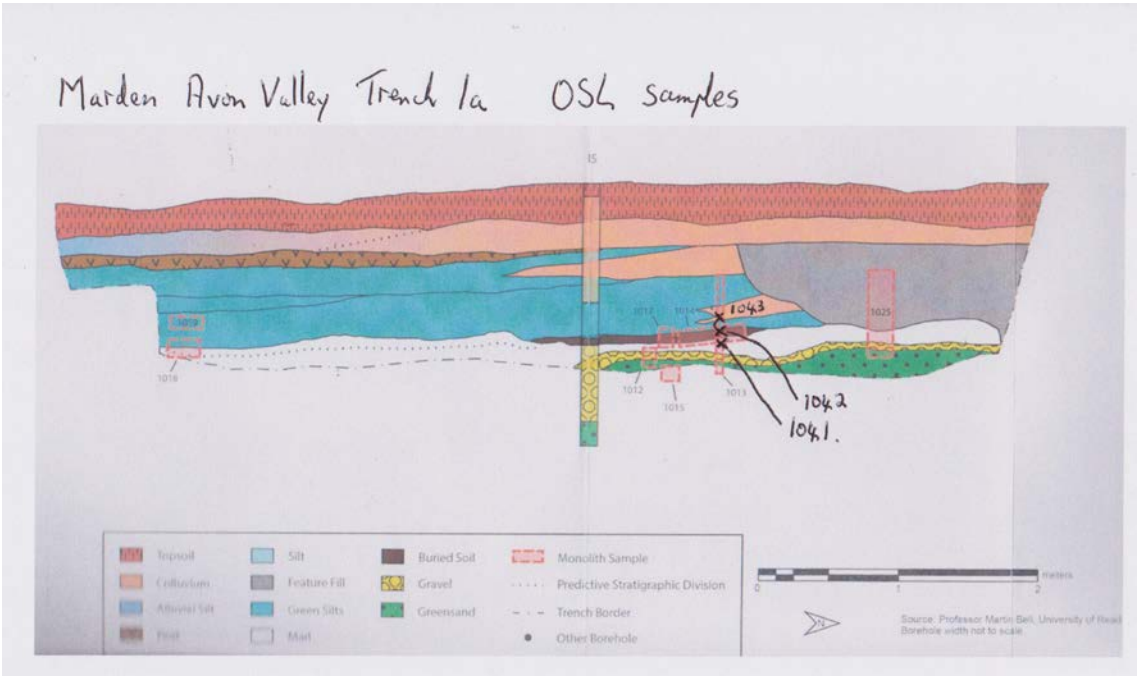

Figure 3. Trench 1a section drawing, showing relative position of the OSL samples

Table 1 D_r, D_e and Age data of the Marden samples located at c. 51°N, 2°W, 105m. Age estimates expressed relative to the year of sampling, 2017. Uncertainties in age are quoted at 1σ confidence, are based on analytical errors and reflect combined systematic and experimental variability and (in parenthesis) experimental variability alone (see § Analytical uncertainty)

Field Code	Lab Code	Overburden (m)	Grain size (μm)	Moisture content (%)	Ge γ-spectrometry (*ex situ*)			β D_r (Gy.ka^{-1})	γ D_r (Gy.ka^{-1})	Cosmic D_r (Gy.ka^{-1})	Preheat (°C for 10s)	Low Dose Repeat Ratio	Interpolated: Applied Low Regenerative-dose D_e	High Dose Repeat Ratio	Interpolated: Applied High Regenerative-dose D_e	Post-IR OSL Ratio
					K (%)	Th (ppm)	U (ppm)									
OSL <1041>	GL17061	1.11	125–180	18±4	1.31±0.09	3.83±0.40	1.72±0.13	1.00±0.12	0.56±0.09	0.18±0.02	260	1.02±0.02	1.02±0.02	1.01±0.02	1.02±0.03	1.00±0.02
OSL <1042>	GL17062	1.02	125–180	20±5	1.23±0.09	4.93±0.41	1.83±0.14	0.96±0.12	0.58±0.09	0.18±0.02	260	1.01±0.02	1.01±0.02	1.02±0.02	1.04±0.02	1.00±0.02
OSL <1043>	GL17063	0.93	125–180	27±7	1.27±0.09	7.39±0.50	1.86±0.14	0.92±0.13	0.61±0.10	0.18±0.02	240	1.00±0.04	1.01±0.03	0.99±0.04	1.00±0.04	0.98± 0.04

Field Code	Lab Code	Total D_r (Gy.ka^{-1})	D_e(Gy)	Age(ka)
OSL <1041>	GL17061	1.73±0.15	25.9±1.0	14.9±1.4 (1.2)
OSL <1042>	GL17062	1.72±0.16	22.8±0.9	13.3±1.3 (1.2)
OSL <1043>	GL17063	1.71±0.19	19.1±1.0	11.2±1.4 (1.3)

Fig. i Signal Calibration

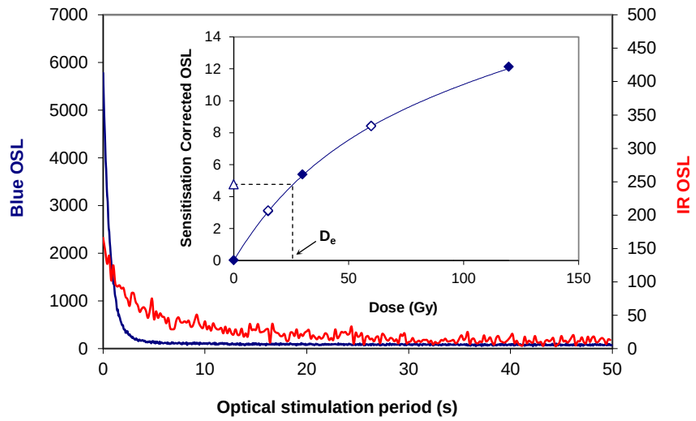

Fig. i Signal Calibration Natural blue and laboratory-induced infrared (IR) OSL signals. Detectable IR signal decays are diagnostic of feldspar contamination. Inset, the natural blue OSL signal (open triangle) of each aliquot is calibrated against known laboratory doses to yield equivalent dose (D_e) values. Repeats of low and high doses (open diamonds) illustrate the success of sensitivity correction.

Fig. ii Dose Recovery

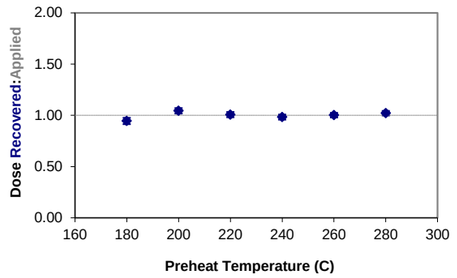

Fig. ii Dose Recovery The acquisition of D_e values is necessarily predicated upon thermal treatment of aliquots succeeding environmental and laboratory irradiation. The Dose Recovery test quantifies the combined effects of thermal transfer and sensitisation on the natural signal using a precise lab dose to simulate natural dose. Based on this an appropriate thermal treatment is selected to generate the final D_e value.

Fig. iii Inter-aliquot D_e distribution

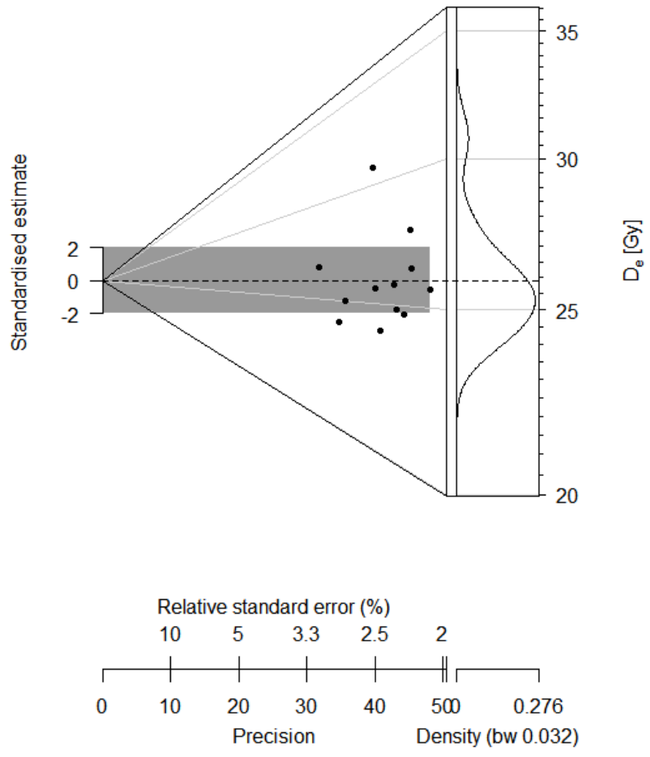

Fig. iii Inter-aliquot D_e distribution Abanico plot of inter-aliquot statistical concordance in D_e values derived from **natural** irradiation. Discordant data (those points lying beyond **±2 standardised ln D_e**) reflect heterogeneous dose absorption and/or inaccuracies in calibration.

Fig. iv Signal Analysis

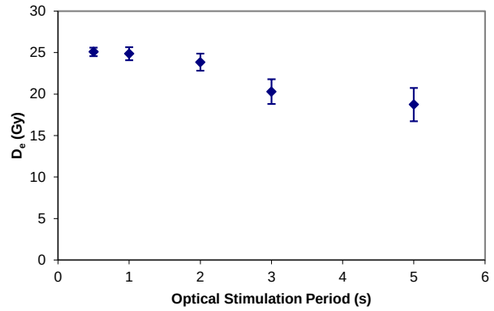

Fig. iv Signal Analysis Statistically significant increase in **natural** D_e value with signal stimulation period is indicative of a partially-bleached signal, provided a significant increase in D_e results from **simulated partial bleaching** followed by insignificant adjustment in D_e for simulated **zero** and **full bleach** conditions. Ages from such samples are considered maximum estimates. In the absence of a significant rise in D_e with stimulation time, simulated partial bleaching and zero/full bleach tests are not assessed.

Fig. v U Decay Activity

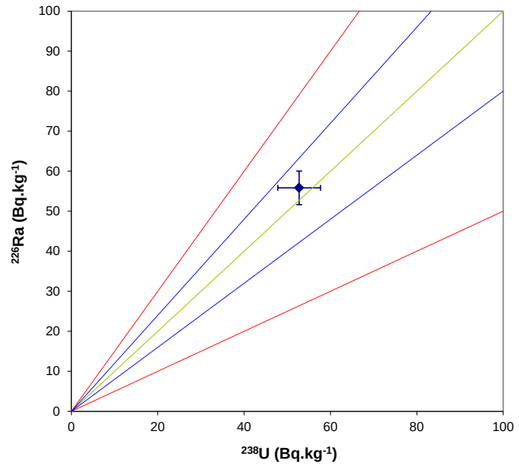

Fig. v U Activity Statistical concordance (equilibrium) in the activities of the daughter radioisotope ^{226}Ra with its parent ^{238}U may signify the temporal stability of D_r emissions from these chains. Significant differences (disequilibrium; >50%) in activity indicate addition or removal of isotopes creating a time-dependent shift in D_r values and increased uncertainty in the accuracy of age estimates. A 20% disequilibrium marker is also shown.

Fig. vi Age Range

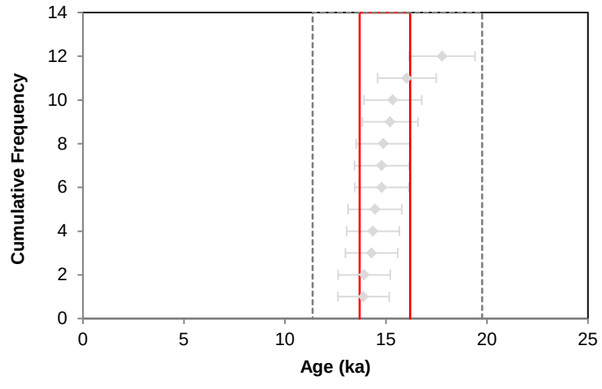

Fig. vi Age Range The Cumulative frequency plot indicates the inter-aliquot variability in age. It also shows the **mean age range**; an estimate of sediment burial period based on mean D_e and D_r values with associated analytical uncertainties. The **maximum influence** of temporal variations in D_r forced by minima-maxima variation in moisture content and overburden thickness is outlined and may prove instructive where there is uncertainty in these parameters. However the combined extremes represented should not be construed as preferred age estimates.

Appendix 1
Sample GL17061

Fig. i Signal Calibration

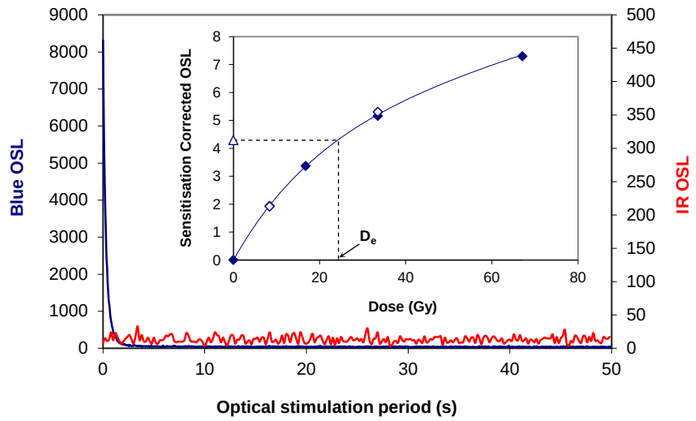

Fig. i Signal Calibration Natural blue and laboratory-induced infrared (IR) OSL signals. Detectable IR signal decays are diagnostic of feldspar contamination. Inset, the natural blue OSL signal (open triangle) of each aliquot is calibrated against known laboratory doses to yield equivalent dose (D_e) values. Repeats of low and high doses (open diamonds) illustrate the success of sensitivity correction.

Fig. ii Dose Recovery The acquisition of D_e values is necessarily predicated upon thermal treatment of aliquots succeeding environmental and laboratory irradiation. The Dose Recovery test quantifies the combined effects of thermal transfer and sensitisation on the natural signal using a precise lab dose to simulate natural dose. Based on this an appropriate thermal treatment is selected to generate the final D_e value.

Fig. iii Inter-aliquot D_e distribution Abanico plot of inter-aliquot statistical concordance in D_e values derived from **natural** irradiation. Discordant data (those points lying beyond ±2 standardised ln D_e) reflect heterogeneous dose absorption and/or inaccuracies in calibration.

Fig. iv Signal Analysis Statistically significant increase in **natural** D_e value with signal stimulation period is indicative of a partially-bleached signal, provided a significant increase in D_e results from **simulated partial bleaching** followed by insignificant adjustment in D_e for simulated **zero** and **full bleach** conditions. Ages from such samples are considered maximum estimates. In the absence of a significant rise in D_e with stimulation time, simulated partial bleaching and zero/full bleach tests are not assessed.

Fig. v U Activity Statistical concordance (equilibrium) in the activities of the daughter radioisotope ^{226}Ra with its parent ^{238}U may signify the temporal stability of D_r emissions from these chains. Significant differences (disequilibrium; >50%) in activity indicate addition or removal of isotopes creating a time-dependent shift in D_r values and increased uncertainty in the accuracy of age estimates. A 20% disequilibrium marker is also shown.

Fig. vi Age Range The Cumulative frequency plot indicates the inter-aliquot variability in age. It also shows the **mean age range**; an estimate of sediment burial period based on mean D_e and D_r values with associated analytical uncertainties. The **maximum influence** of temporal variations in D_r forced by minima-maxima variation in moisture content and overburden thickness is outlined and may prove instructive where there is uncertainty in these parameters. However the combined extremes represented should not be construed as preferred age estimates.

Fig. ii Dose Recovery

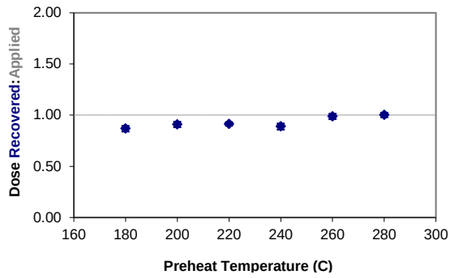

Fig. iii Inter-aliquot D_e distribution

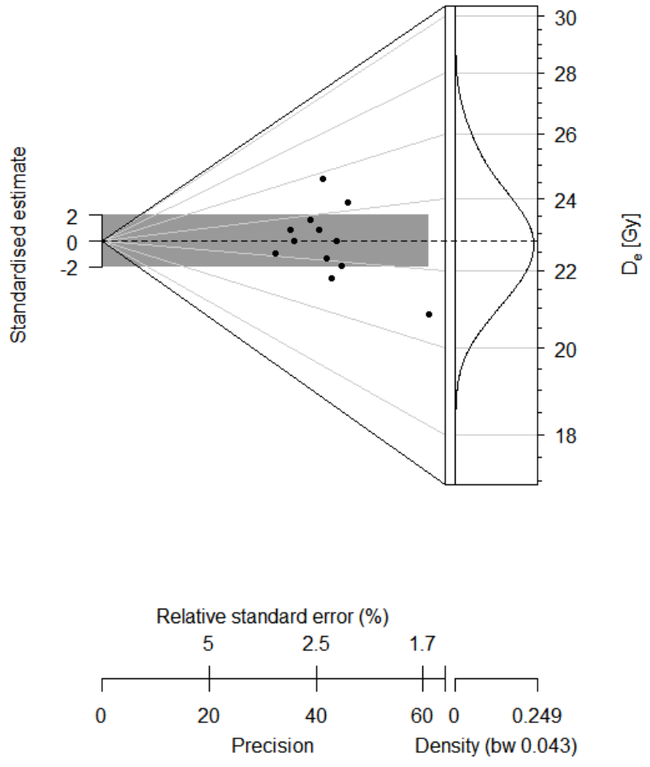

Appendix 2
Sample GL17062

Fig. iv Signal Analysis

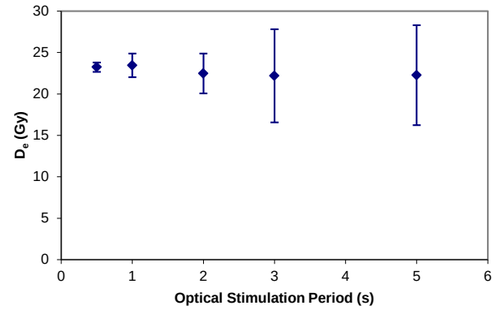

Fig. v U Decay Activity

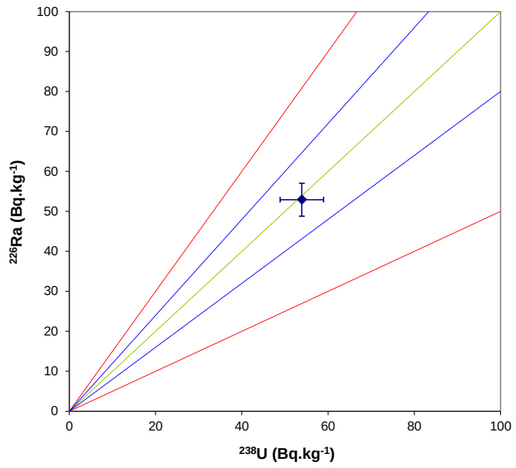

Fig. vi Age Range

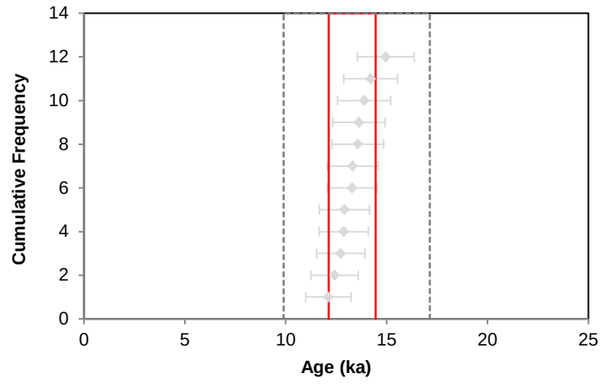

Fig. i Signal Calibration

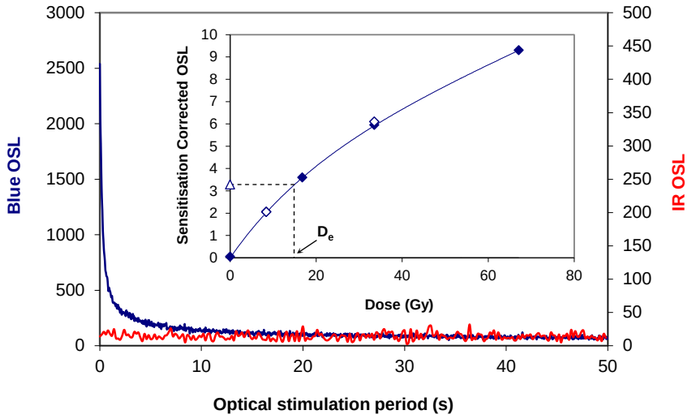

Fig. i Signal Calibration Natural blue and laboratory-induced infrared (IR) OSL signals. Detectable IR signal decays are diagnostic of feldspar contamination. Inset, the natural blue OSL signal (open triangle) of each aliquot is calibrated against known laboratory doses to yield equivalent dose (D_e) values. Repeats of low and high doses (open diamonds) illustrate the success of sensitivity correction.

Fig. ii Dose Recovery The acquisition of D_e values is necessarily predicated upon thermal treatment of aliquots succeeding environmental and laboratory irradiation. The Dose Recovery test quantifies the combined effects of thermal transfer and sensitisation on the natural signal using a precise lab dose to simulate natural dose. Based on this an appropriate thermal treatment is selected to generate the final D_e value.

Fig. iii Inter-aliquot D_e distribution Abanico plot of inter-aliquot statistical concordance in D_e values derived from **natural** irradiation. Discordant data (those points lying beyond **±2 standardised ln D_e**) reflect heterogeneous dose absorption and/or inaccuracies in calibration.

Fig. iv Signal Analysis Statistically significant increase in **natural** D_e value with signal stimulation period is indicative of a partially-bleached signal, provided a significant increase in D_e results from **simulated partial bleaching** followed by insignificant adjustment in D_e for simulated **zero** and **full bleach** conditions. Ages from such samples are considered maximum estimates. In the absence of a significant rise in D_e with stimulation time, simulated partial bleaching and zero/full bleach tests are not assessed.

Fig. v U Activity Statistical concordance (equilibrium) in the activities of the daughter radioisotope ^{226}Ra with its parent ^{238}U may signify the temporal stability of D_r emissions from these chains. Significant differences (disequilibrium; >50%) in activity indicate addition or removal of isotopes creating a time-dependent shift in D_r values and increased uncertainty in the accuracy of age estimates. A 20% disequilibrium marker is also shown.

Fig. vi Age Range The Cumulative frequency plot indicates the inter-aliquot variability in age. It also shows the **mean age range**; an estimate of sediment burial period based on mean D_e and D_r values with associated analytical uncertainties. The **maximum influence** of temporal variations in D_r forced by minima-maxima variation in moisture content and overburden thickness is outlined and may prove instructive where there is uncertainty in these parameters. However the combined extremes represented should not be construed as preferred age estimates.

Fig. ii Dose Recovery

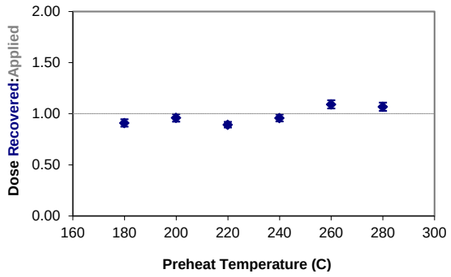

Fig. iii Inter-aliquot D_e distribution

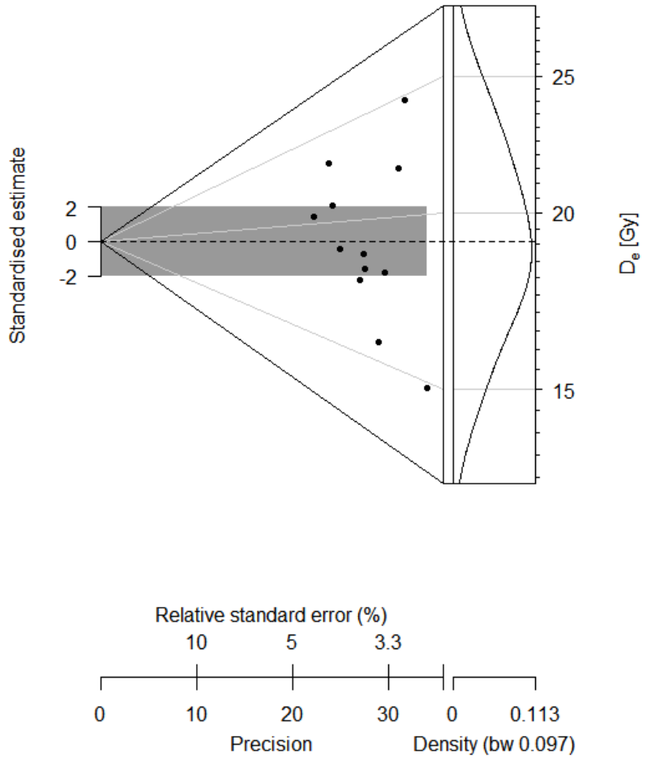

Fig. iv Signal Analysis

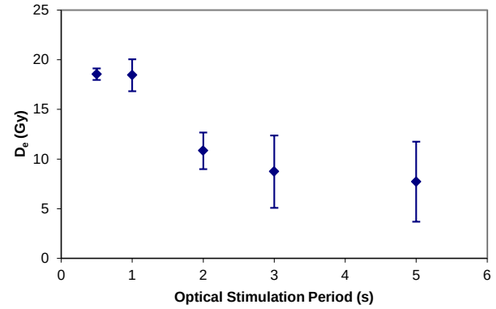

Fig. v U Decay Activity

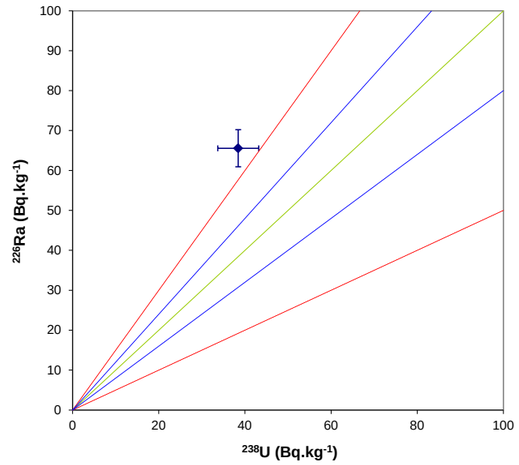

Fig. vi Age Range

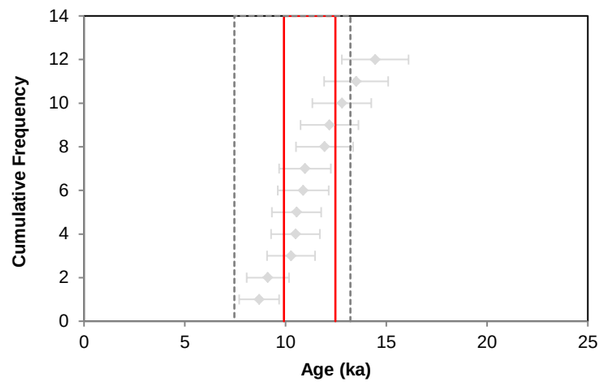

Appendix 3
Sample GL17063

REFERENCES

Adamiec, G and Aitken, M J 1998 'Dose-rate conversion factors: new data'. *Ancient TL* **16**, 37–50

Agersnap-Larsen, N, Bulur, E, Bøtter-Jensen, L and McKeever, S W S 2000 'Use of the LM-OSL technique for the detection of partial bleaching in quartz'. *Radiation Measurements* **32**, 419–25

Aitken, M J 1998 *An introduction to optical dating: the dating of Quaternary sediments by the use of photon-stimulated luminescence*. Oxford: Oxford University Press

Bailey, R M, Singarayer, J S, Ward, S and Stokes, S 2003 'Identification of partial resetting using D_e as a function of illumination time'. *Radiation Measurements* **37**, 511–18

Bateman, M D, Frederick, C D, Jaiswal, M K, and Singhvi, A K 2003 'Investigations into the potential effects of pedoturbation on luminescence dating'. *Quaternary Science Reviews* **22**, 1169–76

Bateman, M D, Boulter, C H, Carr, A S, Frederick, C D, Peter, D and Wilder, M 2007 'Detecting post-depositional sediment disturbance in sandy deposits using optical luminescence'. *Quaternary Geochronology* **2**, 57–64

Berger, G W 2003 'Luminescence chronology of late Pleistocene loess-paleosol and tephra sequences near Fairbanks, Alaska'. *Quaternary Research* **60**, 70–83

Bøtter-Jensen, L, Mejdahl, V and Murray, A S 1999 'New light on OSL'. *Quaternary Science Reviews* **18**, 303–10

Bøtter-Jensen, L, McKeever, S W S and Wintle, A G 2003 *Optically Stimulated Luminescence Dosimetry*. Amsterdam: Elsevier

Dietze, M, Kreutzer, S, Burow, C, Fuchs, M C, Fischer, M and Schmidt, C 2016 'The abanico plot: visualising chronometric data with individual standard errors'. *Quaternary Geochronology* **31**, 1–7

Duller, G A T 2003 'Distinguishing quartz and feldspar in single grain luminescence measurements'. *Radiation Measurements* **37**, 161–65

Field, D, Martin, L and Winton, H 2009 *The Hatfield Earthworks, Marden, Wiltshire, Survey and Investigation*. English Heritage Research Department Report Series **96-2009**

Galbraith, R F, Roberts, R G, Laslett, G M, Yoshida, H and Olley, J M 1999 'Optical dating of single and multiple grains of quartz from Jinmium rock shelter (northern Australia): Part I, Experimental design and statistical models'. *Archaeometry* **41**, 339–64

Gliganic, L A, May, J-H and Cohen, T J 2015 'All mixed up: using single-grain equivalent dose distributions to identify phases of pedogenic mixing on a dryland alluvial fan'. *Quaternary International* **362**, 23–33

Gliganic, L A, Cohen, T J, Slack, M and Feathers, J K 2016 'Sediment mixing in aeolian sandsheets identified and quantified using single-grain optically stimulated luminescence'. *Quaternary Geochronology* **32**, 53–66

Huntley, D J, Godfrey-Smith, D I and Thewalt, M L W 1985 'Optical dating of sediments'. *Nature* **313**, 105–7

Hubbell, J H 1982 'Photon mass attenuation and energy-absorption coefficients from 1keV to 20MeV'. *International Journal of Applied Radioisotopes* **33**, 1269–90

Hütt, G, Jaek, I and Tchonka, J 1988 'Optical dating: K-feldspars optical response stimulation spectra'. *Quaternary Science Reviews* **7**, 381–86

Jacobs, A, Wintle, A G, Duller, G A T, Roberts, R G and Wadley, L 2008 'New ages for the post-Howiesons Poort, late and finale middle stone age at Sibdu, South Africa'. *Journal of Archaeological Science* **35**, 1790–1807

Leary, J and Field, D 2012 'Journeys and juxtapositions. Marden henge and the view from the Vale' in Gibson, A (ed) *Enclosing the Neolithic. Recent studies in Britain and Europe*. Oxford: BAR (International Series 2440), 55–65

Lombard, M, Wadley, L, Jacobs, Z, Mohapi, M and Roberts, R G 2011 'Still Bay and serrated points from the Umhlatuzana rock shelter, Kwazulu-Natal, South Africa'. *Journal of Archaeological Science* **37**, 1773–84

Markey, B G, Bøtter-Jensen, L, and Duller, G A T 1997 'A new flexible system for measuring thermally and optically stimulated luminescence'. *Radiation Measurements* **27**, 83–89

Mejdahl, V 1979 'Thermoluminescence dating: beta-dose attenuation in quartz grains'. *Archaeometry* **21**, 61–72

Murray, A S and Olley, J M 2002 'Precision and accuracy in the Optically Stimulated Luminescence dating of sedimentary quartz: a status review'. *Geochronometria* **21**, 1–16

Murray, A S and Wintle, A G 2000 'Luminescence dating of quartz using an improved single-aliquot regenerative-dose protocol'. *Radiation Measurements* **32**, 57–73

Murray, A S and Wintle, A G 2003 'The single aliquot regenerative dose protocol: potential for improvements in reliability'. *Radiation Measurements* **37**, 377–81

Murray, A S, Olley, J M and Caitcheon, G G 1995 'Measurement of equivalent doses in quartz from contemporary water-lain sediments using optically stimulated luminescence'. *Quaternary Science Reviews* **14**, 365–71

Olley, J M, Murray, A S and Roberts, R G 1996 'The effects of disequilibria in the Uranium and Thorium decay chains on burial dose rates in fluvial sediments'. *Quaternary Science Reviews* **15**, 751–60

Olley, J M, Caitcheon, G G and Murray, A S 1998 'The distribution of apparent dose as determined by optically stimulated luminescence in small aliquots of fluvial quartz: implications for dating young sediments'. *Quaternary Science Reviews* **17**, 1033–40

Olley, J M, Caitcheon, G G and Roberts R G 1999 The origin of dose distributions in fluvial sediments, and the prospect of dating single grains from fluvial deposits using -optically stimulated luminescence. *Radiation Measurements* **30**, 207–17

Olley, J M, Pietsch, T and Roberts, R G 2004 'Optical dating of Holocene sediments from a variety of geomorphic settings using single grains of quartz'. *Geomorphology* **60**, 337–58

Prescott, J R and Hutton, J T 1994 'Cosmic ray contributions to dose rates for luminescence and ESR dating: large depths and long-term time variations'. *Radiation Measurements* **23**, 497–500.

Singhvi, A K, Bluszcz, A, Bateman, M D and Someshwar Rao, M 2001 'Luminescence dating of loess-palaeosol sequences and coversands: methodological aspects and palaeoclimatic implications'. *Earth Science Reviews* **54**, 193–211

Smith, B W, Rhodes, E J, Stokes, S, and Spooner, N A 1990 'The optical dating of sediments using quartz'. *Radiation Protection Dosimetry* **34**, 75–78

Spooner, N A 1993 *The validity of optical dating based on feldspar*. Unpublished D.Phil. thesis, Oxford University

Templer, R H 1985 'The removal of anomalous fading in zircons'. *Nuclear Tracks and Radiation Measurements* **10**, 531–37

Wallinga, J 2002 'Optically stimulated luminescence dating of fluvial deposits: a review'. *Boreas* **31**, 303–22

Wintle, A G 1973 'Anomalous fading of thermoluminescence in mineral samples'. *Nature* **245**, 143–44

Zimmerman, D W 1971 'Thermoluminescent dating using fine grains from pottery'. *Archaeometry* **13**, 29–52

Historic England

Marden Henge, Marden, Wiltshire

Optical Dating of Sediments

Phil Toms, Martin Bell and Jamie Wood

Discovery, Innovation and Science in the Historic Environment

Research Report Series no. 75/2018